

# Structure formation in the quasispherical Szekeres model

Krzysztof Bolejko

*Nicolaus Copernicus Astronomical Center, Polish Academy of Sciences, ul. Bartycka 18, 00-716 Warsaw, Poland\**

(Dated: September 19, 2018)

Structure formation in the Szekeres model is investigated. Since the Szekeres model is an inhomogeneous model with no symmetries, it is possible to examine the interaction of neighboring structures and its impact on the growth of a density contrast. It has been found that the mass flow from voids to clusters enhances the growth of the density contrast. In the model presented here, the growth of the density contrast is almost 8 times faster than in the linear approach.

PACS numbers: 98.65.Dx, 98.65.-r, 98.62.Ai, 04.20.Jb

Keywords: cosmology; structure formation; Szekeres model

## I. INTRODUCTION

Galaxies redshift surveys indicate that our Universe is inhomogeneous. Galaxies form structures like clusters, superclusters, and voids. The most popular methods which are used to describe the evolution of these structures are N-body simulations ([1, 2, 3]) and the linear approach. However, because the present day density contrast is large the linear approach is in most cases inadequate. On the other hand the N-body simulations describe the evolution of large amount of particles which interact gravitationally. However, interactions between particles are described by the Newtonian mechanics. In Newtonian mechanics matter does not affect light propagation, hence within the N-body simulations it is impossible to estimate the influence of matter distribution on light propagation. In general relativity the situation is different, the geometry defined by matter distribution tells the light along which paths to propagate. Thus, in order to have a suitable model which would predict a proper evolution of the density contrast and be adequate to trace light propagation models based on exact solutions of the Einstein equations need to be used. In this paper the Szekeres model is employed to study the evolution of a galaxy supercluster and an adjoining void. The Szekeres model is an exact solution of the Einstein equations, which is inhomogeneous and has no symmetries. Being an exact model of spacetime geometry, the Szekeres model can be adopted not only to describe the evolution of cosmic structures but also to examine light propagation.

The structure of this paper is as follows: Sec. II presents the Szekeres model; in Sec. III B the model of the double-structure is presented; in Sec III C the evolution a void and an adjoining cluster is presented. The results of this evolution are compared with the results obtained in the linear approach and in the inhomogeneous spherically symmetric Lemaître–Tolman model.

## II. THE SZEKERES MODEL

The metric of the Szekeres [4] models is of the following form:

$$ds^2 = dt^2 - e^{2\alpha} dz^2 - e^{2\beta} (dx^2 + dy^2). \quad (1)$$

The components of the metric are as follows:

$$e^\beta = \Phi(t, z) e^{\nu(x, y, z)}, \quad (2)$$

$$e^\alpha = h(z) \Phi(t, z) \beta_{,z}, \quad (3)$$

where  $h(z)$  is an arbitrary function of  $z$ , and  $e^{-\nu}$  is:

$$e^{-\nu} = A(z)(x^2 + y^2) + 2B_1(z)x + 2B_2(z)y + C(z). \quad (4)$$

The functions  $A(z), B_1(z), B_2(z), C(z)$  are not independent but obey the following relation:

$$C(z) = \frac{B_1^2(z)}{A(z)} + \frac{B_2^2(z)}{A(z)} + \frac{1}{4A(z)} \left[ \frac{1}{h^2(z)} + k(z) \right] \quad (5)$$

The Einstein equations reduce to following two:

$$\Phi_{,t}^2(t, z) = \frac{2M(z)}{\Phi(t, z)} - k(z) + \frac{1}{3}\Lambda\Phi^2(t, z), \quad (6)$$

$$\kappa\epsilon = \frac{(2Me^{3\nu})_{,z}}{e^{2\beta}e^{\beta}_{,z}}. \quad (7)$$

In a Newtonian limit  $Mc^2/G$  is equal to the mass inside the shell of radial coordinate  $z$ . However, it is not an integrated rest mass but active gravitational mass that generates a gravitational field.

Eq. (6) can be integrated:

$$\int_0^\Phi \frac{d\tilde{\Phi}}{\sqrt{\frac{2M(z)}{\tilde{\Phi}} - k(z) + \frac{1}{3}\Lambda\tilde{\Phi}^2}} = c[t - t_B(z)], \quad (8)$$

\*Electronic address: bolejko@camk.edu.pl;  
URL: <http://www.camk.edu.pl/~bolejko>

where  $t_B$  appears as an integration constant, and is an arbitrary function of  $z$ . This means that the Big Bang is not a single event as in the Friedmann models, but occurs at different times for different distances from the origin.

As can be seen the Szekeres model is specified by 6 functions. However, by a choice of the coordinates, the number of independent functions can be reduced to 5.

The Szekeres model is known to have no symmetry (Bonnor, Sulaiman and Tomimura [5]). It is of great flexibility and wide application in cosmology (Bonnor and Tomimura [6]), and in astrophysics (Szekeres [7]; Hellaby and Krasiński [8]), and still it can be used as a model of many astronomical phenomena. This paper aims to present the application of the Szekeres model to the process of structure formation.

### A. Coordinate system

The coordinate system in which the metric is of form (1) can be interpreted as a stereographic projection of polar coordinates. This can be seen if the following transformation is considered:

$$\begin{aligned} A &= \frac{1}{2S}, \\ B_1 &= -\frac{P}{2S}, \\ B_2 &= -\frac{Q}{2S}, \\ C &= \frac{P^2}{2S} + \frac{Q^2}{2S} + \frac{S}{2} = \frac{B_1^2}{A} + \frac{B_2^2}{A} + \frac{\varepsilon}{4A}, \\ \varepsilon &= \frac{1}{h^2} + k. \end{aligned} \quad (9)$$

After this transformation we obtain:

$$\begin{aligned} e^{2\nu}(dx^2 + dy^2) &= \\ &= \frac{(dx^2 + dy^2)}{[A(x^2 + y^2) + 2B_1x + 2B_2y + C]^2} = \\ &= \frac{(dx^2 + dy^2)}{\left[\frac{1}{2S}(x^2 + y^2) - 2\frac{P}{2S}x - 2\frac{Q}{2S}y + \frac{P^2}{2S} + \frac{Q^2}{2S} + \frac{S}{2}\right]^2} = \\ &= \frac{(dx^2 + dy^2)}{\frac{S^2}{4} \left[ \left(\frac{x-P}{S}\right)^2 + \left(\frac{y-Q}{S}\right)^2 + \varepsilon \right]^2}. \end{aligned} \quad (10)$$

When  $\varepsilon = 1$  the above transformation is the stereographic projection of a sphere, when  $\varepsilon = 0$  the surface is a plane, and when  $\varepsilon = -1$  it is the stereographic projection of a hyperboloid.

As we are interested in the Friedmann limit of our model, i.e. we expect it becomes an homogeneous Friedmann model in a large distance from the origin, we will focus only on the  $\varepsilon = 1$  case.

Then the transformation of the following form:

$$\begin{aligned} x - P &= S \cot\left(\frac{\theta}{2}\right) \cos(\phi) \\ y - Q &= S \cot\left(\frac{\theta}{2}\right) \sin(\phi) \\ z &= r \end{aligned} \quad (11)$$

leads to:

$$e^{2\beta}(dx^2 + dy^2) = \Phi^2 (d\theta^2 + \sin^2 \theta d\phi^2). \quad (12)$$

After transformation (9) and (11) the metric (1) becomes:

$$\begin{aligned} ds^2 &= cdt^2 - \left\{ \frac{(\Phi_{,r} + \Phi\nu_{,r})^2}{1-k} + \Phi^2 e^{2\nu} \left[ S_{,r}^2 \cot^2 \frac{\theta}{2} \right. \right. \\ &\quad \left. \left. + 2S_{,r} \cot \frac{\theta}{2} (Q_{,r} \sin \phi + P_{,r} \cos \phi) + (P_{,r}^2 + Q_{,r}^2) \right] \right\} dr^2 \\ &\quad - \Phi^2 e^{2\nu} \left[ 2S \cot \frac{\theta}{2} (Q_{,r} \cos \phi - P_{,r} \sin \phi) \right] dr d\phi \\ &\quad + 2\Phi^2 e^\nu \left( Q_{,r} \sin \phi + P_{,r} \cos \phi + S_{,r} \cot \frac{\theta}{2} \right) dr d\theta \\ &\quad - \Phi^2 (d\theta^2 + \sin^2 \theta d\phi^2), \end{aligned} \quad (13)$$

where:

$$e^\nu = \frac{1 - \cos \theta}{S}, \quad (14)$$

and:

$$\nu_{,r} = \frac{S_{,r} \cos \theta + \sin \theta (P_{,r} \cos \phi + Q_{,r} \sin \phi)}{S}. \quad (15)$$

As can be seen, if  $t = \text{const}$ , and  $r = \text{const}$ , the above metric becomes the metric of the 2 dimensional sphere. Hence, every  $t = \text{const}$  and  $r = \text{const}$  slices of the Szekeres  $\varepsilon = 1$  space-time is a sphere. Therefore, the  $\varepsilon = 1$  case is often called quasispherical model. However, as  $S, P$  and  $Q$  are now functions of  $r$ , spheres are not concentric. For the spheres to be concentric, the following conditions must hold:

$$\begin{aligned} P_{,r} &= 0, \\ Q_{,r} &= 0, \\ S_{,r} &= 0. \end{aligned} \quad (16)$$

Such conditions lead to spherical symmetric case, and the metric (13) becomes the line element of the Lemaitre-Tolman model [9, 10].

## B. The Friedmann limit

The Friedmann limit is an essential element of our model. The model presented in this paper describes the evolution of a void with an adjoining cluster in the expanding Universe. Far away from the origin density and velocity distributions tend to the values that they would have in a Friedmann model. Consequently the values of the time instants and values of the density and velocity fluctuations are calculated with respect to this homogeneous background.

The Friedmann limit follows when:

$$\Phi(r, t) = R(r)f(t), \quad (17)$$

$$k(r) = -k_0 R^2(r), \quad (18)$$

where  $k_0$  is the curvature index of the FLRW models.

The above conditions are sufficient to obtain the homogeneous FLRW model, and the metric (1) assumes the Goode and Wainwright [11] form of the FLRW model. Then from Eq. (7) follows:

$$M(r) = M_0 R^3(r), \quad (19)$$

where  $M_0$ , expressed by FLRW parameters is  $M_0 = (1/2)(\Omega_m H_0^2/c^2)$ . Inserting the above into Eq. (8) it follows that  $t_B(r) = \text{const}$ , which implies that the Big Bang was simultaneous. Although, the metric in polar coordinates (13) is still not diagonal, under the transformation (16), the metric obtains a more usual form:

$$ds^2 = dt^2 - \frac{f^2(t)}{1 - k_0 R^2} dR^2 - R^2 f^2(t) d\Omega^2, \quad (20)$$

where  $d\Omega^2 = d\theta^2 + \sin^2\theta d\phi^2$ .

## III. STRUCTURE FORMATION

This paper aims to present the application of the Szekeres model to the process of structure formation. In this section the model of an evolving void with adjoining supercluster is presented. As will be seen the use of Szekeres model gives better understanding of the structure formation, and shows the importance of voids in process of cluster formation.

The model is expected to remain consistent with the astronomical data. As mentioned in Sec. II B the density fluctuations, as well as time instants are calculated with respect to the homogeneous background model. The chosen background model is the FLRW model with the density:

$$\rho_b = \Omega_m \times \rho_{cr} = 0.3 \times \frac{3H_0^2}{8\pi G}. \quad (21)$$

The Hubble constant is of  $H_0 = 72 \text{ km s}^{-1} \text{ Mpc}^{-1}$ , and the cosmological constant corresponds to  $\Omega_\Lambda = 0.7$ , where  $\Omega_\Lambda = (1/3)(c^2\Lambda/H_0^2)$ .

Below the density distribution and the evolution of a void and an adjoining cluster is calculated. It can be seen from Eqs. (7), (14), and (15) that to calculate the density distribution for any instant  $t_i$ , one needs to now 5 functions:  $M(r)$ ,  $S(r)$ ,  $Q(r)$ ,  $P(r)$ , and  $\Phi(t_i, r)$ . The explicit forms of these functions are presented below. Using these functions the density distribution of the present day structures can be calculated (see Sec. III B). Then, the evolution of the system can be traced back in time. The density distribution depends on time only via the function  $\Phi(t, r)$  and its derivative. The value of the  $\Phi(t, r)$  for any instant can be calculated by solving the differential equation [see Eq. (6)]. In most cases, as in this paper, this equation can be solved only numerically. To solve this equation one needs to know the initial conditions:  $\Phi(t_0, r)$ , and the functions  $M(r)$ , and  $k(r)$  as well as the value of  $\Lambda$ . This equation was solved numerically using the fourth-order Runge–Kutta method [12]. Knowing the value of  $\Phi(t, r)$  for any instant the density distribution can be calculated as described above.

### A. Observational constrains

Astronomical observations show that in small scales matter distribution and expansion of the space are not homogeneous. The measurements of matter distribution imply that density varies from  $\rho \approx 0.06\rho_b$  in voids [13] to  $\rho$  equal several tens of background density ( $\rho_b$ ) in clusters [14]. These structures are of diameters from several Mpc up to several tens of Mpc. However, if the averaging is considered on large scales, the density varies from  $0.3\rho_b$  to  $4.4\rho_b$  [15, 16], and the structures are of several tens of Mpc.

### B. Model of a void with an adjoining supercluster

As mentioned above, to specify the model one needs to know 5 functions of the radial coordinate. Let us define the radial coordinate as a current value of  $\Phi$ :

$$r := \Phi(z, t_0) \quad (22)$$

Three out of these five unknown functions can be  $P(r)$ ,  $Q(r)$ ,  $S(r)$ . However the physically important quantities are not these functions, but their gradients. If  $P(r)$ ,  $Q(r)$ ,  $S(r)$  are constant, then as can be seen from Eqs. (15), (14) and Eq. (7), the density distribution and the evolution Eq. (6) do not depend on them. Then the Szekeres model becomes the Lemître–Tolman model. The explicit forms of these functions are presented in next subsections. The next two functions can be either,  $t_B(r)$ ,  $M(r)$ ,  $k(r)$  or any other combination of functions, from which these can be calculated. The function  $M(r)$

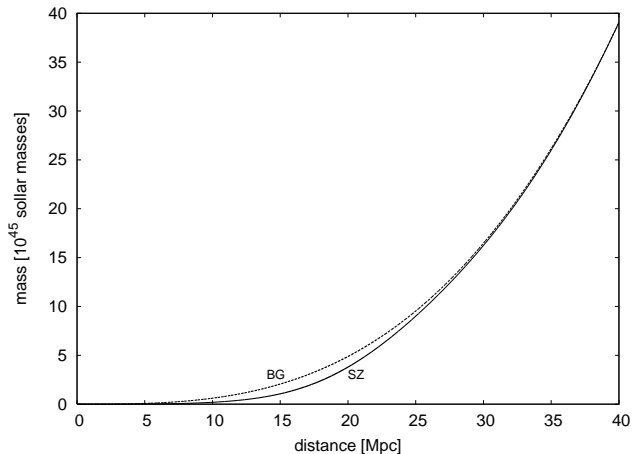


FIG. 1: The mass distribution within the homogeneous background (BG) and in the Szekeres model (SZ).

describes the active gravitational mass inside the  $t = \text{const}$ ,  $r = \text{const}$  sphere. The assumed mass distribution is presented in Fig. 1. The void is placed at the origin, so the mass of the model in Fig. 1 is below the background mass, but then it is compensated by more dense regions, and soon, at the distance of about 30 Mpc, the mass distribution becomes goes over into the homogeneous background. To define the model we need one more function. Let us assume that the bang time function is constant and equal to zero. Then from Eq. (8) the function  $k(r)$  can be calculated.

### 1. Model 1

As mentioned above, if the functions  $P(r)$ ,  $Q(r)$  and  $S(r)$  are constant, the quasispherical Szekeres model becomes a Lemaitre–Tolman model. Let us then consider the simplest generalisation of the Lemaitre–Tolman model. Let us focus on a model with  $S(r)$  and  $P(r)$  being constant, and  $Q(r)$  being chosen as below.

Let us choose:

$$\begin{aligned} S &= 140, \\ P &= 10, \\ Q &= -113 \ln(1 + r). \end{aligned} \quad (23)$$

The density distribution was calculated from Eq. (7), and it is presented in Figs. 2(a) — 2(d). Fig. 2(a) presents a schematic view of the structure. Fig. 2(b) and Fig. 2(c) depict the horizontal cross section through the equator ( $Z = 0$ ), so it goes through the void and the cluster [as presented in Fig. 2(a)]. Fig 2(d) depicts the vertical ( $X = 0$ ) cross section, so it goes through the void and the cluster [as presented in Fig. 2(a)].

It should be stressed that the shapes presented in Figs. 2(b) — 2(d), are a bit distorted in comparison with the

real density distribution. The Szekeres model describes the density distribution in a curved space, and it is impossible to map it into a 2 dimensional flat surface (such as a sheet of this paper). This problem is similar to drawing maps of our globe.

### 2. Model 2

Let us consider the following functions:

$$\begin{aligned} S &= -r^{0.59}, \\ P &= 0.83 \times r^{0.59}, \\ Q &= 0.4 \times r^{0.59}. \end{aligned} \quad (24)$$

The density distribution is presented in Figs. 3(a) — 3(f). Fig. 3(a) presents a schematic view of the structure. Fig 3(b) depicts the vertical cross section, so it goes through the void and the cluster [as presented in Fig. 3(a)]. Figs. 3(c) and 3(d) show the cross section through the equator ( $Z = 0$ ) while Figs. 3(e) and 3(f) depict the cross section through the surface of  $Z = -20$  Mpc [it passes through the cluster presented in Fig. 3(b)].

As can be seen, this model does not qualitatively differ from model 1. Both models present mass distributions similar to dipole structure. It is well known that the mass distribution in the Szekeres model has the form of a mass-dipole superposed on a monopole. This was first noticed by Szekeres [7]. The functions  $S$ ,  $P$ , and  $Q$  simply describe the position of this dipole. As can be seen from Eq. (15), the functions  $P$ , and  $Q$  cause that the density distribution [eq. (7)] changes periodically with the period  $2\pi$ . Although  $\nu, r$  appears in the denominator as well as in the numerator of Eq. (7), it is impossible to have the period larger than  $2\pi$  because it would introduce shell crossing singularities (see Hellaby and Krasiński [8]; Plebański and Krasiński [17] for details on how to avoid shell crossings in the Szekeres model). The function  $S(r)$  on the other hand, as seen from Eq. (15) describes the dipole distribution along vertical axis. By setting  $S$ ,  $P$ , and  $Q$  constant we drag the dipole to the origin and smooth it out to a spherically symmetric mass distribution.

The shell crossing, which was mentioned above, can also occur during the evolution. Sometimes it can be avoided by suitable choice of the initial data, but there are situations when it is impossible and the Szekeres model breaks down. This means that pressure cannot be neglected and a more realistic matter model should be employed. (It is expected that in those more realistic models, for which no exact solutions of Einstein's equations are known so far, the shell crossings would be replaced by regions of high density. These large densities would become infinite in the limit of zero pressure gradient.) However, in models presented here, matter density is not extreme and diameters of considered structures are

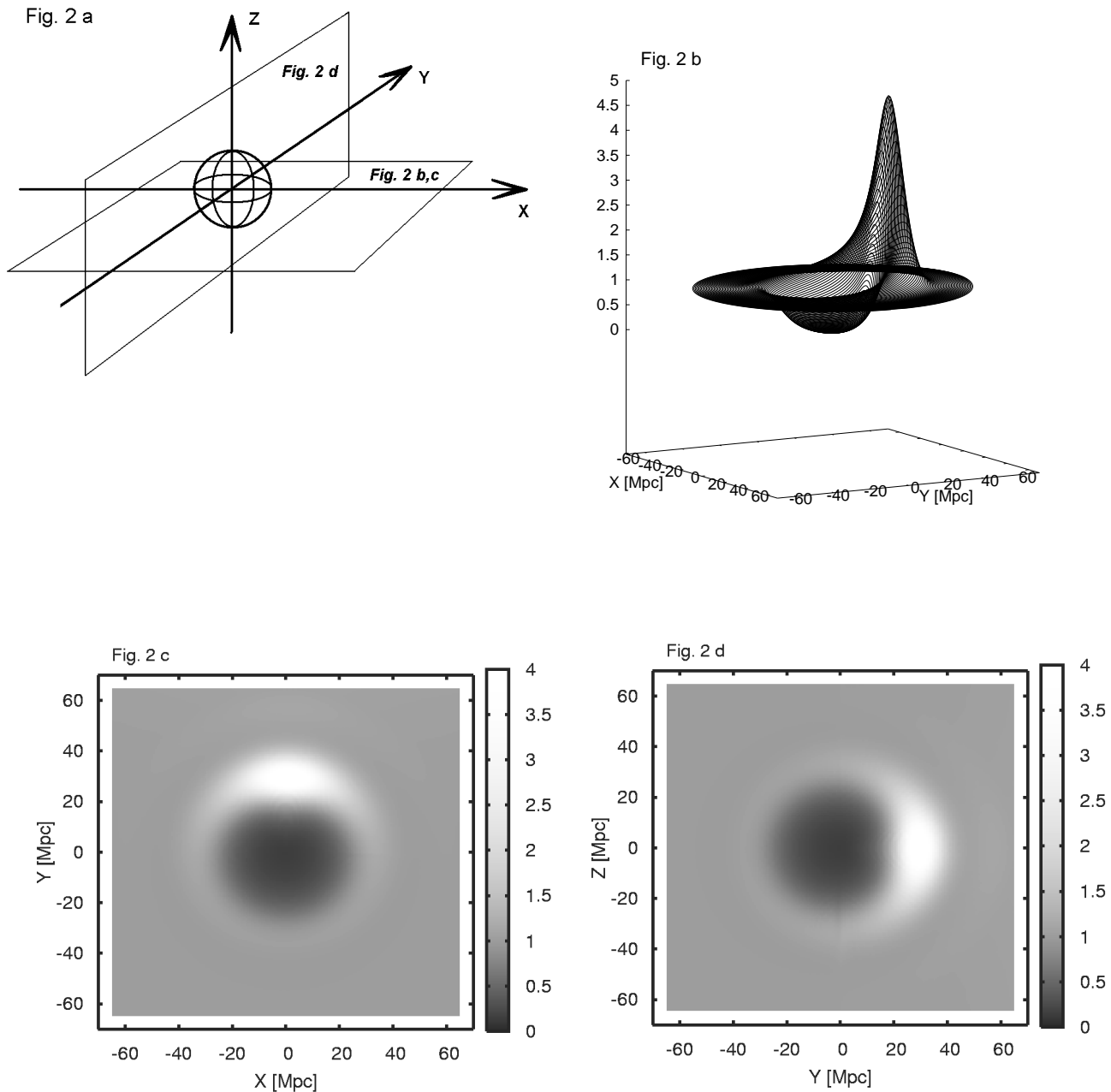


FIG. 2: (“to editor: for online version please use color figures: fig2c\_col.eps and fig2d\_col.eps”) The present day density distribution of model 1 (Sec. III B 1). Fig. 2(a) presents a schematic view. Figs. 2(b) – 2(d) presents the density distribution in background units. Coordinates  $X, Y, Z$  are defined as follows:  $X = \Phi(t_0, r) \sin \theta \cos \phi$ ,  $Y = \Phi(t_0, r) \sin \theta \sin \phi$ ,  $Z = \Phi(t_0, r) \cos \theta$ .

large, thus the Szekeres model is appropriate and employing a more sophisticated model with inhomogeneous pressure distribution is unnecessary.

### C. Evolution

Since model 1 does not differ significantly from the 2, let us focus only on the evolution of model 1. The evolution of the model is presented in Fig. 4. Fig. 4 shows

the evolution of a density profile which goes through the void and the cluster, it is the line  $Z = X = 0$  presented in Fig. 2(a) — 2(d). The density distribution is presented for different instants, from 100 million years after the Big Bang up to the present.

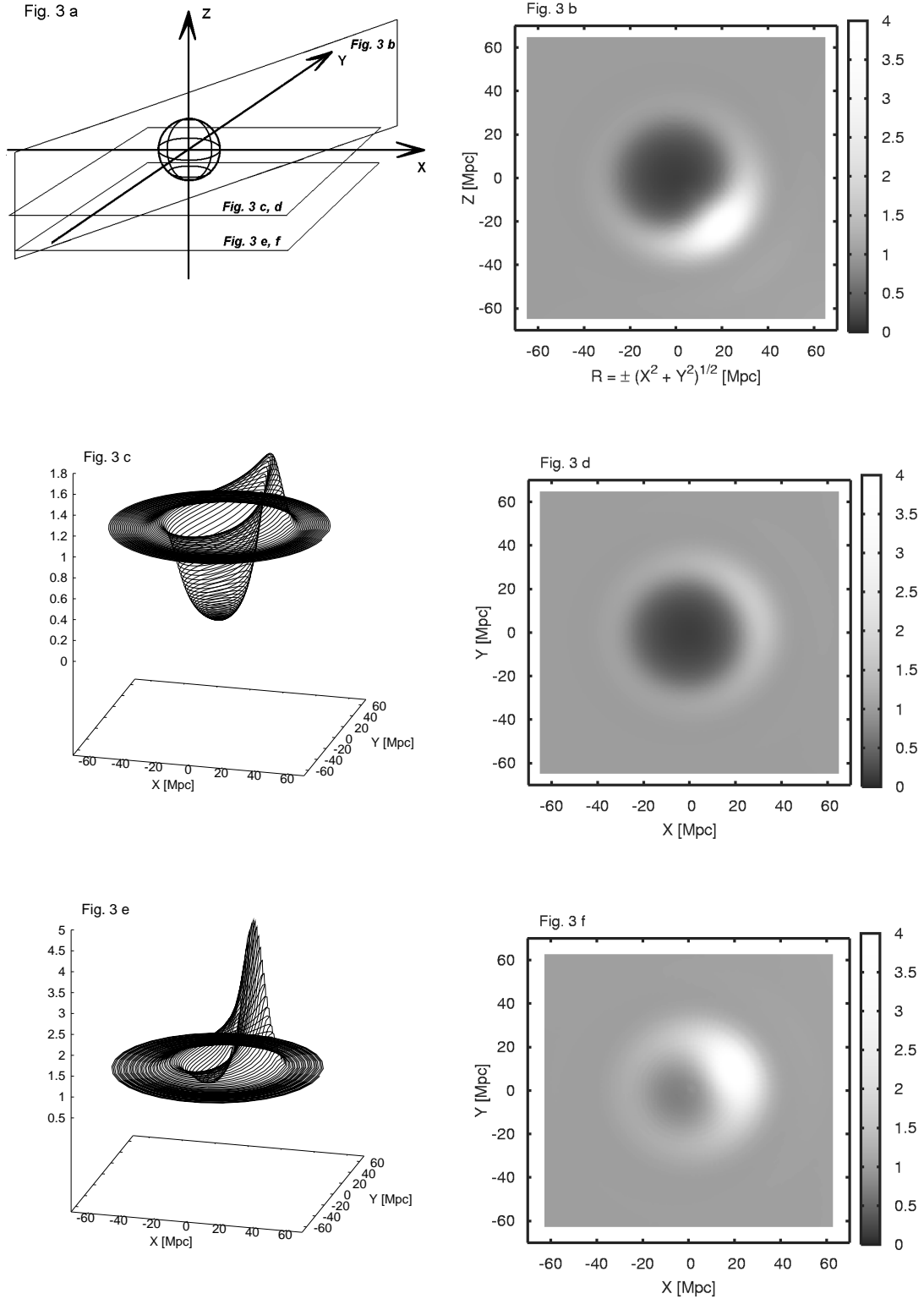


FIG. 3: ("to editor: for online version please use color figures: fig3b\_col.eps,fig3d\_col.eps, and fig3f\_col.eps") The present day density distribution of model 1 (Sec. III B 2). Fig. 3(a) presents a schematic view. Figs. 3(b) – 3(f) presents the density distribution in background units. Coordinates  $X, Y, Z$  are defined as follows:  $X = \Phi(t_0, r) \sin \theta \cos \phi$ ,  $Y = \Phi(t_0, r) \sin \theta \sin \phi$ ,  $Z = \Phi(t_0, r) \cos \theta$ .

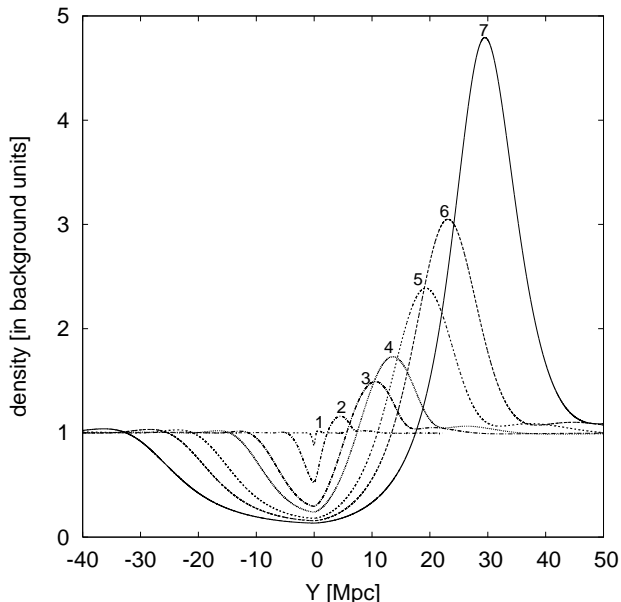


FIG. 4: The density profile for different time instants: 1 — 100 My after the Big Bang, 2 — 1 Gy, 3 — 3.5 Gy, 4 — 5 Gy, 5 — 8 Gy, 6 — 10 Gy, 7 — present instant.

### 1. Comparison of different approaches

To estimate how two neighboring structures influence each other's evolution, let us compare the evolution of the double structure presented above with the evolution of single structures obtained by other models. The usual way of calculating the evolution of a density contrast is the linear approach. The linear approach is based on the assumption that the density evolves like in a homogeneous background but with a small correction:

$$\rho(r, t) = \rho_b [1 + \delta(r, t)], \quad (25)$$

Inserting the above formula into the Einstein equations and after linearising the equations, one obtains:

$$\ddot{\delta} + 2\frac{\dot{a}_b}{a_b}\dot{\delta} - \frac{1}{2}\kappa c^2\rho_b\delta = 0 \quad (26)$$

However, due to the large present density contrast, this approach is in most cases inadequate. An alternative approach is to use the spherical symmetric Lemaître–Tolman model. Since it is an exact and inhomogeneous solution of the Einstein equations, one does not have to worry about the smallness of the present day density contrast. The density contrast is defined similarly as above:

$$\delta(r, t) = \frac{\rho(r, t) - \rho_b}{\rho_b}. \quad (27)$$

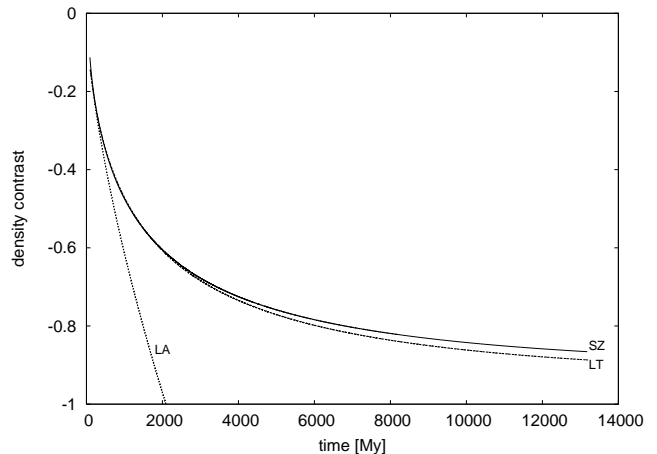


FIG. 5: The evolution of the density contrast inside the void within the Szekeres model (SZ), the Lemaître–Tolman model (LT) and the linear approach (LA).

The evolution of cosmic structures in the Lemaître–Tolman model was studied in detail by Krasiński and Hellaby [18, 19, 20], Bolejko, Krasiński & Hellaby [21].

The comparison of the evolution of the density contrast in the Szekeres and Lemaître–Tolman models, and in the linear approach is presented in Figs. 5 and 6. These figures present the values of the density contrast at central parts of a void (Fig. 5) and a cluster (Fig. 6). The initial conditions specifying these models were the same as in the Szekeres model. The initial instant was 100 million years after the Big Bang.

Fig. 5 presents the evolution of the density contrast inside the void. As one can see the linear approach becomes inadequate very soon, and after 2 Gy it gives unphysical values (the density contrast cannot be smaller than  $-1$ ). The evolutions of the density contrast in the Szekeres and Lemaître–Tolman models are comparable, although the Lemaître–Tolman produces lower values. In the Lemaître–Tolman model mass flows from the central part in all directions with the same rate. In the Szekeres model the mass-flow depends on the direction, hence this small difference in final values of the density contrast. The feature of the mass-flow's direction and its significance is more visible in the cluster evolution's case.

Fig. 6 presents the evolution of the density contrast inside the cluster. As one can see, the evolutions of the density contrast in the linear approach and Lemaître–Tolman model are comparable. The evolution of the density contrast in the Szekeres model is significantly faster. This implies that the adjoining void plays a significant role in the process of the cluster formation. The mass-flow from the void towards the cluster is much faster than from other directions. This can be seen as an asymmetry of a void. This asymmetry is clearly depicted in Fig 4.

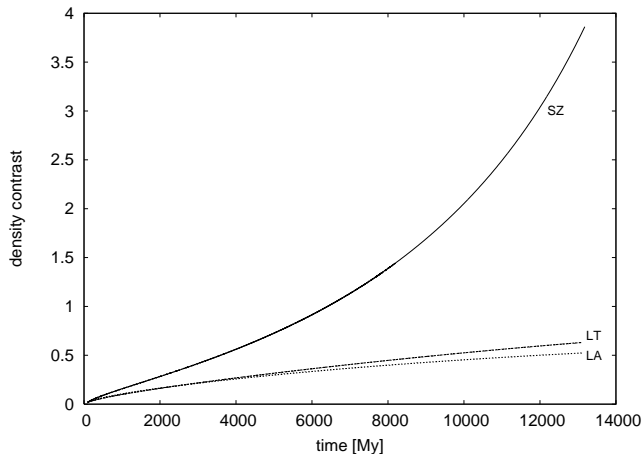


FIG. 6: The evolution of the density contrast inside the cluster within the Szekeres model (SZ), the Lemaître–Tolman model (LT) and the linear approach (LA).

#### IV. CONCLUSIONS

This paper presents the application of the Szekeres model to the process of structure formation. A model of a double structure, i.e. a void with an adjoining supercluster was constructed. Since this model is based on an exact solution of Einstein’s equations, it presets the evolution of these structures without such approximations as linearity, hence the interaction between described struc-

tures can be estimated.

The results show that the mass flow from the void to the cluster enhances the growth of the density contrast of a galaxy cluster. In the model presented here the growth of the density contrast was about 5 times faster than in a spherically symmetric model, and 8 times faster than in the linear approach. The evolution of the voids is similar to the evolution in the Lemaître–Tolman model but because the spherical models do not distinguish any direction, the outward mass flow is a little bit faster than in the Szekeres model. As seen in Figs. 5 — 6, the process of the structure formation is a strongly nonlinear process.

The models based on the Szekeres solution have also one more advantage. They can be used in problems of light propagation, which is impossible in the N-body simulations. The Szekeres model has still a great, but so far unused, potential for applications in cosmology, and in the future might be of great importance in modeling some processes.

#### Acknowledgments

I would like to thank Andrzej Krasiński and Charles Hellaby for their valuable comments and discussions concerning the Szekeres model. Andrzej Krasiński is gratefully acknowledged for his help with preparing the manuscript.

- 
- [1] V. Springel et al. *Nature* **435**, 629 (2005)
  - [2] J. M. Colberg et al. *Mon. Not. R. Astron. Soc.*, **319**, 209 (2000)
  - [3] A. Jenkins et al. *Astrophys. J* **499**, 20 (1998)
  - [4] P. Szekeres, *Commun. Math. Phys.* **41**, 55 (1975a).
  - [5] W. B. Bonnor, A. H. Sulaiman, and N. Tomimura, *Gen. Relativ. Gravit.* **8**, 549 (1977).
  - [6] W. B. Bonnor and N. Tomimura, *Mon. Not. R. Astron. Soc.* **175**, 85 (1976).
  - [7] P. Szekeres, *Phys. Rev. D* **12**, 2941 (1975b).
  - [8] C. Hellaby and A. Krasiński, *Phys. Rev. D* **66**, 084011 (2002).
  - [9] G. Lemaître, *Ann. Soc. Sci. Bruxelles* **A53**, 51 (1933); reprinted in *Gen. Relativ. Gravit.* **29**, 641 (1997).
  - [10] R. C. Tolman, *Proc. Nat. Acad. Sci. USA* **20**, 169 (1934); reprinted in *Gen. Relativ. Gravit.* **29**, 935 (1997).
  - [11] S. W. Goode and J. Wainwright, *Phys. Rev. D* **26**, 3315 (1982).
  - [12] W. H. Press, B. P. Flannery, S. A. Teukolsky, and W. T. Vetterling, *Numerical Recipes. The art of Scientific Computing* (Cambridge Univ. Press, Cambridge, 1986).
  - [13] F. Hoyle and M. S. Vogeley, *Astrophys. J.* **607**, 751 (2004).
  - [14] S. Bardelli, F. Zucca, G. Zamorani, L. Moscardini, and R. Scaramella, *Mon. Not. R. Astron. Soc.* **312**, 540 (2000).
  - [15] T. Kolatt, A. Dekel, and O. Lahav, *Mon. Not. R. Astron. Soc.* **275**, 797 (1995).
  - [16] M. J. Hudson, *Mon. Not. R. Astron. Soc.* **265**, 43 (1993).
  - [17] J. Plebański and A. Krasiński, *Introduction to general relativity and cosmology* (Cambridge Univ. Press, Cambridge, in press).
  - [18] A. Krasiński and C. Hellaby, *Phys. Rev. D* **65**, 023501 (2002).
  - [19] A. Krasiński and C. Hellaby, *Phys. Rev. D* **69**, 023502 (2004).
  - [20] A. Krasiński and C. Hellaby, *Phys. Rev. D* **69**, 043502 (2004).
  - [21] K. Bolejko, A. Krasiński and C. Hellaby, *Mon. Not. R. Astron. Soc.* **362**, 213 (2005).